Asociación Argentina
de Mecánica Computacional

Mecánica Computacional Vol XXIX, págs. 473-492 (artículo completo)
Eduardo Dvorkin, Marcela Goldschmit, Mario Storti (Eds.)
Buenos Aires, Argentina, 15-18 Noviembre 2010

TOPOLOGY OPTIMIZATION WITH *h*-ADAPTIVE REFINEMENT PROCESS IN THERMOELASTIC BIDIMENSIONAL PROBLEMS

João C. A. Costa Jr.[a], Marcelo K. Alves[b], Paulo S. R. da Silva[c] and Hilbeth P. A de Deus[d]

[a] *UFRN – Federal University of Rio Grande do Norte, Campus Universitário, Lagoa Nova, Centro Tecnológico, Depto. de Eng. Mecânica, CEP 59072-790, Natal – RN, Brazil, arantes@ufrnet.br, http://www.dem.ufrn.br.*

[b] *UFSC – Federal University of Santa Catarina, Campus Universitário, Trindade, Centro Tecnológico, Cx. Postal - 476, CEP 88040-900, Florianópolis – SC, Brazil, krajnc@emc.ufsc.br, http://www.gmac.ufsc.br.*

[c] *IFBA – Federal Institute of Bahia, Campus de Salvador, Salvador – BA, Brazil, http://www.portal.ifba.edu.br.*

[d] *UTFPR – Federal Technological University of Paraná, Campus Curitiba, DAMEC - Departamento Acadêmico de Mecânica, NuMAT, Av. Sete de Setembro, 3165, CEP 80230-901, Rebouças, Curitiba – PR, Brazil, azikri@utfpr.edu.br, http://www.numat.ct.utfpr.edu.br. PPGEM-UTFPR/PPGMNE-UFPR.*

Keywords: *topology optimization, thermoelasticity, FEM, adaptivity, error estimator.*

Abstract. This work proposes a formulation for optimization of bidimensional (2D) structure layouts submitted to mechanic and thermal shipments and applied an h-adaptive filter process which conduced to computational low spend and high definition structural layouts. The main goal of the formulation is to minimize the structure mass submitted to an effective state of stress of von Mises, with stability and lateral constraint variants. A criterion of global measurement was used for intents a parametric condition of stress fields. To avoid singularity problems was considerate a release on the stress constraint. On the optimization was used a material approach where the homogenized constructive equation was function of the material relative density. The intermediary density effective properties were represented for a Solid Isotropic Microstructures with Penalization (SIMP) type artificial model. The problem was simplified by use of the method of finite elements of Galerkin using triangles with linear Lagrangian basis. On the solution of the optimization problem, was applied the augmented Lagrangian Method, that consists on minimum problem sequence solution with box-type constraints, resolved by a second order projection method which uses the method of the quasi-Newton without memory, during the problem process solution. This process reduces computational expends showing be more effective and solid. The results materialize more refined layouts with accurate topologic and shape of structure definitions. On the other hand formulation of mass minimization with global stress criterion provides to modeling "ready" structural layouts, with violation of the criterion of homogeneous distributed stress.

1 INTRODUCTION

The reduction of the cost of manufacturing a given component or product may be obtained by applying some optimization tool. In the particular case of components or products obtained by an injection process (plastic or metal powder), the possibility to consider complex geometry allow us to explore the flexibility of the process by designing optimized molds with an optimum topology for the domain of the component.

One of the most difficult decisions in the designing phase is to specify the layout of the geometry of the component. Once the layout or topology of the component is defined we may concentrate in the definition of the optimum shape of the domain, sizing of some additional geometric parameters used to define the model and some material properties, (Suzuki and Kikuchi, 1990; Suzuki and Kikuchi, 1991; Bendsoe and Kikuchi, 1998; Bendsoe, 1995).

In general, the appropriate choice of the layout is strongly dependent of the designer, what implies in the necessity of a designer with a large practical experience. The decision process associated with the definition of the optimum layout of component may be done automatically by employing a topology optimization software, (Bendsoe and Sigmund, 2003; Bendsoe and Rodrigues, 1991; Bendsoe et al. 1993).

In this work, the layout optimization is done by considering a Solid Isotropic Microstructure with Penalization (SIMP). The material density function ρ are the design parameters and varies continuously from 0 to 1, taking the value of 1.0 for a solid material and 0.0 for a void material, Costa Jr. and Alves (2003). To avoid numerical singularity, the lower bound of material, $\rho_{\min}$, is introduced as

$$0 < \rho_{\min} \le \rho \le 1 . \tag{1}$$

2 FORMULATION OF THE PROBLEM

2.1 Determination of the Thermo Mechanical Problem

The thermal problem considered in this work is illustrated in Figure 1.

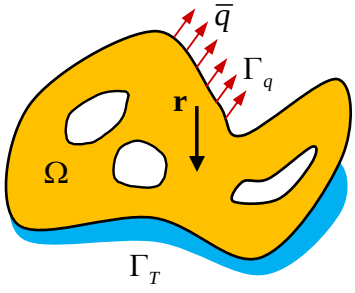

Fig. 1: Definition of the Thermal Problem.

Here $\partial\Omega = \Gamma_T \cup \Gamma_q$; $\Gamma_T \cap \Gamma_q = \varnothing$. Denoting by Γ_T and Γ_q the part of the boundary where the temperature and the heat flux are prescribed respectively. At this point, we define the set of admissible temperatures, W_T, and the set of the temperature variations, Var_T, to be given as: $W_T = \left\{ T \,\middle|\, T \in H^1(\Omega) :\ T = \bar{T} \text{ at } \Gamma_T \right\}$ and $Var_T = \left\{ \hat{T} \,\middle|\, \hat{T} \in H^1(\Omega) :\ \hat{T} = 0 \text{ at } \Gamma_T \right\}$, where $\bar{T}$ is a prescribed temperature imposed over the temperature boundary Γ_T. We consider the

source/sink to be given by a convection heat transfer from the body to a fluid, *i. e.*, $r = -h(T - T_\infty)$ where T_∞ denotes the temperature of the fluid and h the convection heat transfer coefficient. Notice that, if $T > T_\infty$ then heat is removed from the body and if $T < T_\infty$ heat is given to the body, (Alves and Alves, 1999; Silva, 2007).

The weak formulation of the thermal problem may be stated as: Let $T = T^* + T_p$, where $T_p \in W_T$ is a known field. The problem consists in the determination of $T^* \in Var_T$ such that,

$$a_T(T^*, \hat{T}) = l_T(\hat{T}), \quad \forall \hat{T} \in Var_T \tag{2}$$

where

$$a_T(T^*, \hat{T}) = \int_\Omega \mathbf{K}^H \nabla T^* \cdot \nabla \hat{T}\, d\Omega + \int_\Omega h T^* \hat{T}\, d\Omega \tag{3}$$

and

$$l_T(\hat{T}) = \int_\Omega h(T_\infty - T_p)\hat{T} d\Omega + \int_{\Gamma_q} \bar{q}\, \hat{T} d\Gamma - \int_\Omega \mathbf{K}^H \nabla T_p \cdot \nabla T d\Omega \tag{4}$$

Here, the conductivity matrix $\mathbf{K}^H = k^H \mathbf{I}$, where k^H is the homogenized thermal conductivity of the material that is porous material dependent, such that

$$k^H = \rho^\eta k \tag{5}$$

where k is the conductivity parameter for the fully density material, ρ the relative density material and η is the SIMP penalty parameter, (Cho and Choi, 2005; Rodrigues and Fernandes, 1993).

The mechanical problem considered in this work is illustrated in Figure 2.

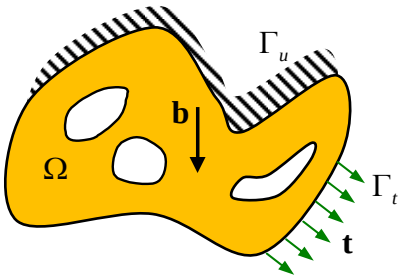

Fig. 2: Definition of the Mechanical Problem.

Here $\partial\Omega = \Gamma_u \cup \Gamma_t$; $\Gamma_u \cap \Gamma_t = \varnothing$. Here, Γ_u and Γ_t represent the part of the boundary where the displacement and the traction are prescribed respectively. At this point we define the set of admissible displacements, W_u, and the set of the displacement variations, Var_u, to be given as: $W_u = \left\{ \mathbf{u} \middle| \mathbf{u} \in [H^1(\Omega)]^3 : \mathbf{u} = \bar{\mathbf{u}} \text{ at } \Gamma_u \right\}$ and $Var_u = \left\{ \mathbf{v} \middle| \mathbf{v} \in [H^1(\Omega)]^3 : \mathbf{v} = 0 \text{ at } \Gamma_u \right\}$. Here, for simplicity we consider $\bar{\mathbf{u}} = 0$. As a result, $W_u = Var_u$.

The weak formulation of the mechanical problem may be stated as: Let $T \in W_T$ be the solution of the problem. Then, the problem consists in the determination of $\mathbf{u} \in W_u$ such that

$$a_u(\mathbf{u},\mathbf{v}) = l_u(\mathbf{v}), \quad \forall \mathbf{v} \in Var_u . \tag{6}$$

where

$$a_u(\mathbf{u},\mathbf{v}) = \int_\Omega \sigma(\mathbf{u}) \cdot \varepsilon(\mathbf{v}) d\Omega , \tag{7}$$

$$l_u(\mathbf{v}) = \int_\Omega \mathbf{b} \cdot \mathbf{v}\, d\Omega + \int_{\Gamma_t} \mathbf{t} \cdot \mathbf{v}\, d\Gamma , \tag{8}$$

and been T_0 the reference temperature of the body

$$\sigma(\mathbf{u}) = \mathbf{D}^H \varepsilon(\mathbf{u}) - (T - T_0)\mathbf{B}^H \tag{9}$$

Now, since we consider the material (matrix) to be isotropic, we have:

$$B_{ij} = B_0 \delta_{ij}, \qquad B_0 = \frac{E\alpha}{1-2\nu} . \tag{10}$$

Here, α is the linear thermal expansion coefficient, $(T - T_0) B_{ij}$ is the thermal stress tensor and $\mathbf{D}$ is the generalized Hooke's law for a linear elastic body, (Brahim-Otsmane *et al.*, 1989; Francfort, 1983). Moreover,

$$D_{ijrs} = \lambda \delta_{ij} \delta_{rs} + \mu(\delta_{ir}\delta_{js} + \delta_{is}\delta_{jr}) \tag{11}$$

with

$$\lambda = \frac{\nu E}{(1-\nu)(1-2\nu)}, \qquad \mu = G = \frac{E}{2(1-\nu)} . \tag{12}$$

Where λ and μ are the Lame´s constants, ν is the Poisson´s ratio and E is the Young modulus.

The constitutive matrix $\mathbf{D}^H$ adapted to intermediary density material, proposed by Cho and Choi (2005) is given

$$\mathbf{D}^H_{ijkl} = \rho^\eta \mathbf{D}_{ijkl} . \tag{13}$$

2.2 Formulation of the Problem

The objective of this work is to determine the optimum layout of the structure obtained as solution to an optimization problem. The optimization problem consists in the minimization of the mass of the structure subjected to an effective von Mises equivalent stress and side constraints. The design variable is the relative density of the material, represented by ρ, for dealing with the problem of stress criteria in mass minimization was used SIMP exponential penalty system to describe the constitutive relation of the material, which is used $\eta = 3$, with this choice, proposed by Sigmund and Petersson (1998), we get a description of feasible microstructure material.

The problem may than be formulated as:

$$\min_{\rho(x)} \int_{\Omega} \rho \, d\Omega, \tag{14}$$

such that

$$\sigma_{eq}^{*}\left(\rho(\mathbf{x}), \mathbf{u}\left(\rho(\mathbf{x}), \mathbf{x}, T\right), T\right) - \sigma_y \leq 0 \tag{15}$$

$$\rho_{\inf} - \rho \leq 0 \tag{16}$$

$$\rho - \rho_{\sup} \leq 0, \qquad \forall \mathbf{x} \in \Omega \tag{17}$$

where u(a) and T(a) are obtained as a solution to the problem:

$$a_T(T^*, \hat{T}) = l_T(\hat{T}), \qquad \forall \hat{T} \in Var_T \tag{18}$$

$$a_u(\mathbf{u}, \mathbf{v}) = l_u(\mathbf{v}), \qquad \forall \mathbf{v} \in Var_u \tag{19}$$

and $T = T^* + T_p$, for a given $T_p \in W_T$. The effective von Mises stress, for this microstructure is considered to be given as:

$$\sigma_{eq}^{*} = \frac{\sigma_{eq}}{\rho^{\eta}}. \tag{20}$$

The Karush-Kuhn-Tucker necessary optimality conditions associated with this problem is given by: Let $L(\bullet)$ denote the lagrangian functional associated with the problem, *i. e.*,

$$\begin{aligned} L(\rho, \mathbf{u}, T^*, \lambda_\sigma, \lambda_i, \lambda_s) = & \int_{\Omega} \rho \, d\Omega + \int_{\Omega} \lambda_\sigma \left(\sigma_{eq}^{*}(\rho, \mathbf{u}(\rho, \mathbf{x}, T^*), T^*) - \sigma_y\right) d\Omega \\ & + \int_{\Omega} \lambda_i (\rho_{\inf} - \rho) \, d\Omega + \int_{\Omega} \lambda_s (\rho - \rho_{\sup}) \, d\Omega \end{aligned}, \tag{21}$$

where λ_σ, λ_i, and λ_s are the Lagrange multipliers associated with the inequality constraints, Costa Jr. and Alves (2003). Then, the optimality conditions are given by:

$$\lambda_\sigma \geq 0, \qquad \lambda_{\mathrm{i}} \geq 0, \qquad \lambda_{\mathrm{s}} \geq 0, \tag{22}$$

$$\lambda_\sigma (\sigma_{eq} - \sigma_y) = 0, \qquad \lambda_{\mathrm{i}} (\rho_{\inf} - \rho) = 0, \qquad \lambda_{\mathrm{s}} (\rho - \rho_{\sup}) = 0, \tag{23}$$

$$\sigma_{eq} - \sigma_y \leq 0, \qquad \rho_{\inf} - \rho \leq 0, \qquad \rho - \rho_{\sup} \leq 0 \quad \text{and} \tag{24}$$

$$1 + \lambda_\sigma \frac{\partial \sigma_{eq}^{*}}{\partial \rho} - \lambda_i + \lambda_s = 0, \qquad \forall \mathbf{x} \in \Omega. \tag{25}$$

2.3 Stress Singularity Problem

In order to open the degenerated parts of the design space with the possibility of creating or removing holes without violating the effective stress constraint we apply the κ- relaxation technique (Duysinx, 1998; Duysinx and Sigmund, 1998; Duysinx and Bendsoe, 1998). In this work, we implement an automatic and systematic strategy to reduce the initial perturbation

parameter κ. The stress relaxation parameter is decremented as we get closer to the solution. Now, let $\rho_{\text{sup}} = 1$ be the relative density associated with the full material condition. Then, knowing that $\mathbf{u} = \mathbf{u}\left(\rho(\mathbf{x}), \mathbf{x}, T\right)$, the relaxed admensionalized effective stress constraint may be written as:

$$g\left(\rho(\mathbf{x}), \mathbf{u}, T\right) = \rho(\mathbf{x})\left(\frac{\sigma_{eq}^{*}\left(\rho(\mathbf{x}), \mathbf{u}, T\right)}{\sigma_y} - 1\right) + \kappa\left(\rho_{\text{sup}} - \rho(\mathbf{x})\right) \leq 0\,. \tag{26}$$

From this consideration, the relaxed minimization problem may be formatted as:

$$\min_{\rho} \int_{\Omega} \rho \, d\Omega \tag{27}$$

such that

$$\rho\left(\frac{\sigma_{eq}^{*}}{\sigma_y} - 1\right) + \kappa(\rho_{\text{sup}} - \rho) \leq 0 \tag{28}$$

$$\rho_{\text{inf}} - \rho \leq 0 \tag{29}$$

$$\rho - \rho_{\text{sup}} \leq 0, \qquad \forall\, \mathbf{x} \in \Omega \tag{30}$$

3 DISCRETIZATION OF THE PROBLEM

In order to solve the thermo-mechanical problem we apply the Galerkin Finite Element Method. Moreover, we consider the material density associated with each finite element linearly distributed. Consequently, the material properties related to given element are characterized by a single microstructure. Thus, for each element we have a design variable “a” which represents the size of the void of the microstructure that fully represents the given finite element material properties. From this consideration, the number of design variables is given by the number of finite elements in the mesh.

Furthermore, we make use of the slope-constrained conditions proposed by Petersson and Sigmund (1998). These conditions are employed in order to ensure the existence of a solution to the layout optimization problem and to eliminate the well-known checkerboard instability problem (Bendsoe, 1995; Sigmund and Petersson, 1998), that occur in the Galerkin finite element discretization, when using a low order interpolation base function, in the approximation space. Thus,

$$\left(\frac{\partial \rho}{\partial x}\right)^2 \leq C_x^2 \tag{31}$$

and

$$\left(\frac{\partial \rho}{\partial y}\right)^2 \leq C_y^2 \tag{32}$$

Here, the constants C_x and C_y define the bounds for the components of the gradient of the relative density. These bounds are imposed component wise with the objective of properly imposing a symmetry condition, which may be used in some particular cases.

The discretized problem may be formulated as:

$$\min_{\rho} \int_{\Omega} \rho \, d\Omega \tag{33}$$

such that

$$\frac{\sigma_{eq}^{*}\left(\rho(\mathbf{x}),\mathbf{u}\left(\rho(\mathbf{x}),\mathbf{x},T\right),T\right)}{\sigma_y} + \kappa\left(\frac{1}{\rho_0}-\frac{1}{\rho}\right)-1 \le 0, \quad \forall \mathbf{x} \in \Omega \tag{34}$$

and

$$\rho_{\inf} - \rho_i \le 0\,, \tag{35}$$

$$\rho_i - \rho_{\sup} \le 0, \qquad i=1,...,n \ \text{(number of nodes in the mesh)} \tag{36}$$

3.1 Global Stress Condition

Notice that, the effective stress constraint is a parametric constraint that must be satisfied for $\forall \mathbf{x} \in \Omega$. In order to handle this parametric constraint we relax the pointwise criteria and consider a global integrated constraint. This can be done by replacing a parametric constraint of the type

$$g\left(\rho(\mathbf{x}),\mathbf{u}\left(\rho(\mathbf{x}),\mathbf{x},T\right),T^{*}\left(\rho\right)\right) \le 0, \quad \forall \mathbf{x} \in \Omega \tag{37}$$

by the following associated global constraint:

$$\overline{g}\left(\rho(\mathbf{x}),\mathbf{u}\left(\rho(\mathbf{x}),\mathbf{x},T\right),T^{*}\left(\rho\right)\right) = \left\{\frac{1}{\Omega}\int_{\Omega}\left\langle \rho(\mathbf{x}),\mathbf{u}\left(\rho(\mathbf{x}),\mathbf{x},T\right),T^{*}\left(\rho\right)\right\rangle^{p} d\Omega\right\}^{1/p} = 0\,. \tag{38}$$

Here, in order to enforce the point wise constraint we must consider $p \to +\infty$. However, for practical purposes we consider $p = 2$ where $\langle g(\bullet)\rangle$ denotes the positive part of the function g(•), *i. e.*, $\langle g(\bullet)\rangle = \max\{0, g(\bullet)\}$, Silva (2007).

3.2 Formulation of the Discretized Problem

The discretized formulation of the relaxed problem may be stated as: Determine $\boldsymbol{\rho} \in \wp$, with $\wp = \left\{\boldsymbol{\rho} \in \mathbb{R}^n \,\middle|\, \rho_i^{\inf} \le \rho_i \le \rho_i^{\sup}, i = 1,\ldots,n\right\}$, where n is the total number of nodes, so that it is the solution of:

$$\min_{\boldsymbol{\rho}} \int_{\Omega} \boldsymbol{\rho} \, d\Omega\,. \tag{39}$$

such that

$$\overline{g}\left(\rho(\mathbf{x}),\mathbf{u},T^*(\rho)\right)=\left\{\frac{1}{\Omega}\int_{\Omega}\left\langle g(\rho(\mathbf{x}),\mathbf{u},T^*(\rho)\right\rangle^p d\Omega\right\}^{1/p}=0, \tag{40}$$

$$\rho_{\inf}-\rho_i\le 0, \tag{41}$$

$$\rho_i-\rho_{\sup}\le 0, \qquad i=1,...,n. \tag{42}$$

$$g_{2e-1}(\rho)=\frac{1}{\beta}\left[\left(\frac{\partial\rho}{\partial x}\right)^2-C_x^2\right]\le 0, \tag{43}$$

$$g_{2e}(\rho)=\frac{1}{\beta}\left[\left(\frac{\partial\rho}{\partial y}\right)^2-C_y^2\right]\le 0, \quad e=1,\ldots,n_e, \tag{44}$$

denoting by n_e is the total number of elements. The values $\mathbf{u}(\boldsymbol{\rho})$ and $T^*(\boldsymbol{\rho})$ are the solution of:

$$a_T(T^*,\hat{T})=\rho_T(\hat{T}), \qquad \forall\,\hat{T}\in Var_T^n\subset Var_T \quad \text{and} \tag{45}$$

$$a_u(\mathbf{u},\mathbf{v})=l_u(\mathbf{v}), \qquad \forall\,\mathbf{v}\in Var_u^n\subset Var_u \tag{46}$$

4 MESH REFINEMENT AND ADAPTIVITY

4.1 General description of the method

The objective, here, is to describe the new proposed procedure which combines the topology optimization and the *h*-adaptive finite element methods. The main relevant advantages of the procedure are: the improvement of the definition of the material contour, the reduction of the number of design variables and the decrease of the error of the solution of the state equation.

The procedure is defined by setting a priori the total number of *h*-refinement levels and to solve, at each level, a topology optimization problem. A general description of the algorithm is given as follows:

1. Initialize the design variables
2. Read the data and generate the initial finite element data structure
3. For each *h*-refinement level, do:
   - 3.1. Solve the layout optimization problem
   - 3.2. Apply the mesh refinement procedure
     - 3.2.1. Get the mesh data structure
     - 3.2.2. Perform the mesh refinement
       - 3.2.2.1. Identify which elements must be refined
       - 3.2.2.2. Perform the refinement of the elements and introduce the necessary transition elements in order to maintain the mesh compatibility
       - 3.2.2.3. Apply a constrained Laplacian smoothing procedure in order to improve the mesh quality

3.2.3. Optimize the element nodal incidence for the profile reduction
3.2.4. Update the mesh and finite element data structure

4.2 Mesh Refinement Strategy

The objective at this point is to determine the subset of all elements in the mesh that will be refined. Once this subset is defined, an introduction of the transition elements is performed in order to maintain the mesh compatibility. The refined and transition elements are illustrated in Figure 3 and Figure 4, the set of refined elements may be obtained with the usage of a pointer Pref(*i*), *i*=1…*n*. The default value is Pref(*i*)=0 representing no action. However, if Pref(*i*)=1 then we refine the i-th element. The mesh refinement strategy may be described as follows:

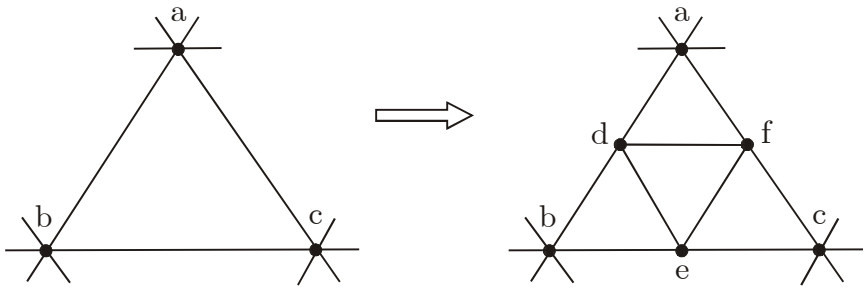

(a) Initial element (b) Refined element

Figura 3: Scheme of refinement of the element Tri3.

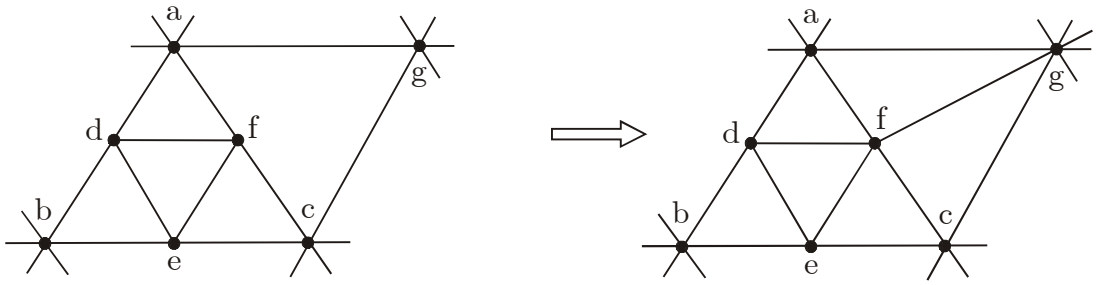

Figura 4: Scheme of transition element.

1. Set Pref=0.
2. Determine the global and the elements average errors denoted respectively by Θ_{GE} and Θ_E, *e*=1…*n*. Now, for each element we verify if $\Theta_E > (1+\eta)\Theta_{GE}$, for some given $\eta > 1$. If true, we set Pref(*e*)=1, *i.e.*, the *e*-th element will be refined.
3. Determine the quality measure *Q* of each element in the mesh, given by

$$Q = \frac{6A}{\sqrt{3}\, L_{\max} P} \tag{47}$$

where

A is the area of the triangle

P is the one half of the perimeter of the triangle

$L_{\max} = \max\left\{\overrightarrow{ab}, \overrightarrow{ac}, \overrightarrow{bc}\right\}$ is the length of the element's largest side

Also, for each element we verify if $Q(e) \le 0.55$. If true, we set Pref(*e*)=1.

4. Identify all the elements which have a face common with the material contour and set their pointer reference Pref(*e*)=1.
5. Perform an additional smoothing refinement criterion. Here, for each element whose

Pref(e)=0 we identify their neighbors. If the element has 2 or more neighbors whose Pref(.)=1, then refine the given element, i.e., set Pref(e)=1.

4.3 Material boundary identification

The objective here is to define a criterion for the definition of the material boundary contour and to refine the elements that have a face common to the given identified material contour. A description of the procedure is given as follows:

1. For each element, e=1...n, do:
1.1. If the relative density of the element, ρ_{E}, is such that $\rho_{\mathrm{E}} > \beta$, $\beta \in (0.5,1)$ then
  1.1.1. Get the element neighbors list associated with the e-th element.
  1.1.2. For each of k-th neighbor elements do:
    1.1.2.1. If $\rho_k < (1-\beta)$ then set both Pref(e)=1 and Pref(k)=1.

As a result, this procedure refines all the elements whose relative density $\rho_{\mathrm{E}} > \beta$ and also the elements whose relative density $\rho_{\mathrm{E}} < \beta$ but have at least a side that forms the material boundary.

4.4 Additional smoothing refinement criteria

The objective here is to avoid having a given non-refined element having 2 or more neighbors to be refined. This may lead to the generation of sharp edges in the material contour or may lead to the generation of internal void regions with a poor material contour definition. As a result, we refine these elements.

4.5 Conditional Laplacian smoothing procedure

In order to improve the mesh, after the refinement step, we employ a constrained Laplacian smoothing, which is illustrated in Figure 5. Here, n is the number of adjacent nodes associated with node x_n.

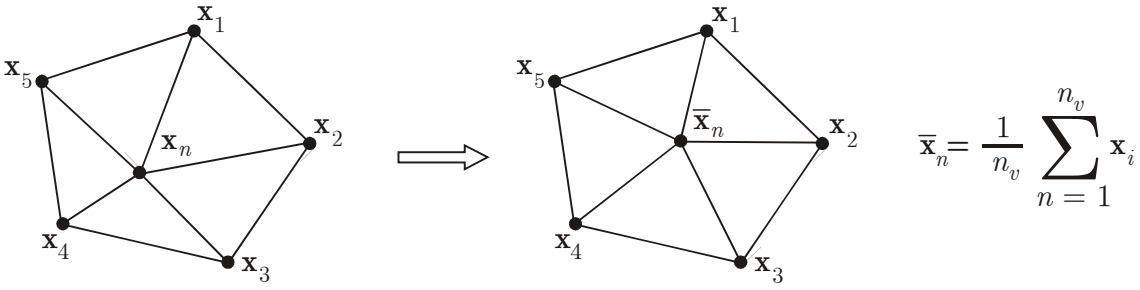

Figura 5: Laplacian Smoothing Scheme.

The Laplacian process is conditional since it will only be implemented if the mesh quality of the set of elements, as illustrated in Figure 5, improves. The mesh quality of the set of elements is given by the quality of the worst element in the set. The measure of quality of a given element is given by eqn. (47).

As a result, the refinement strategy may be summarized as: A given element is refined if,

(i) The measure of the quality of the element is smaller than a given lower bound;

(ii) The element has a side which forms the material boundary of the given topology of the domain;
(iii) The error estimate is larger than a relative prescribed value.

Once these elements are defined we also refine the elements which have two or more elements to be refined, obtained by the application of the criteria in (i), (ii) and (iii).

4.6 Error Estimator and refinement criteria

Here, for simplicity, we employ an error estimator based on the work of Zienkiewics and Zhu (1990, 1991). Notice, however, that the constitutive equation depends on the relative density of the material and that the relative density field is considered as a constant field within the element domain but discontinuous across different elements. As a result of this consideration, we obtain a discontinuous stress field. Thus, in order to apply the Zienkiewics and Zhu approach we make use of the strain field. Hence, the modified method estimates the discretization error of the problem using a gradient recovery technique, now in terms of the strain field, by means of the energy norm. Let $\boldsymbol{\rho}$ be a given realizable distribution of the relative density of the material. Then, the local displacement error may be defined as:

$$\mathbf{e}(\boldsymbol{\rho}) = \mathbf{u}(\boldsymbol{\rho}) - \mathbf{u}_h(\boldsymbol{\rho}) \tag{48}$$

where $\boldsymbol{u}(\boldsymbol{\rho})$ is the exact solution and $\mathbf{u}_h(\boldsymbol{\rho})$ is the approximate solution of the problem. Then, the energy norm may be written as:

$$\left\| e(\boldsymbol{\rho}) \right\|_{\mathrm{E}}^2 = \int_{\Omega} D^H(\boldsymbol{\rho}) \varepsilon\left(\mathbf{e}(\boldsymbol{\rho})\right) \cdot \varepsilon\left(\mathbf{e}(\boldsymbol{\rho})\right) d\Omega \ . \tag{49}$$

Thus, the local strain error may be expressed in terms of the local displacement error as follows:

$$\mathbf{e}_{\varepsilon}(\boldsymbol{\rho}) = \varepsilon(\boldsymbol{\rho}) - \varepsilon_h(\boldsymbol{\rho}) = \varepsilon\left(\mathbf{u}(\boldsymbol{\rho})\right) - \varepsilon\left(\mathbf{u}_h(\boldsymbol{\rho})\right) \tag{50}$$

and the energy norm may be written as:

$$\left\| \mathbf{e}(\boldsymbol{\rho}) \right\|_{\mathrm{E}}^2 = \int_{\Omega} \left[D^H(\boldsymbol{\rho}) \right] \left(\varepsilon(\boldsymbol{\rho}) - \varepsilon_h(\boldsymbol{\rho}) \right) . \left(\varepsilon(\boldsymbol{\rho}) - \varepsilon_h(\boldsymbol{\rho}) \right) d\Omega \, . \tag{51}$$

Since the exact strain distribution is unknown, we approximate $\varepsilon(\boldsymbol{\rho})$ by an improved solution $\varepsilon^*(\boldsymbol{\rho})$, which is more refined then $\varepsilon_h(\boldsymbol{\rho})$. Thus, the error indicator is approximated by:

$$\left\| \mathbf{e}(\boldsymbol{\rho}) \right\|_{\mathrm{E}}^2 = \int_{\Omega} \left[D^H(\boldsymbol{\rho}) \right] \left(\varepsilon^*(\boldsymbol{\rho}) - \varepsilon_h(\boldsymbol{\rho}) \right) . \left(\varepsilon^*(\boldsymbol{\rho}) - \varepsilon_h(\boldsymbol{\rho}) \right) d\Omega \, . \tag{52}$$

Determination of $\varepsilon^*(\boldsymbol{\rho})$

In order to determine the improved solution, $\varepsilon^*(\boldsymbol{\rho})$, we apply the same projection technique proposed by Zienkiewicz and Zhu (1990, 1991) but now based on the fact that the finite element solution $\mathbf{u}_h(\boldsymbol{\rho}) \in C^0(\Omega)$ and that the strain field is only piece-wise continuous. The determination of $\varepsilon^*(\boldsymbol{\rho})$ consists in the solution of the least square minimization of the potential $\psi(\boldsymbol{\rho})$, given by

$$\psi(\boldsymbol{\rho}) = \int_{\Omega} \left\| \varepsilon^*(\boldsymbol{\rho}) - \varepsilon_h(\boldsymbol{\rho}) \right\|^2 d\Omega \tag{53}$$

Here, $\varepsilon^*(\boldsymbol{\rho})$ is interpolated within each element as

$$\varepsilon^* = \sum_{k=1}^{n} N_i \, \overline{\varepsilon}_i^* \tag{54}$$

where $\overline{\varepsilon}_i^*$ represents the vector of strain components, evaluated at the *i*-th node of the element, and N_i are the classical finite element interpolation functions.

At this point, once $\varepsilon^*(\boldsymbol{\rho})$ is determined, we may compute global average error, Θ_{GE}, as:

$$\Theta_{\mathrm{GE}} = \frac{1}{\Omega} \int_{\Omega} \left[D^H(\boldsymbol{\rho}) \right] \left(\varepsilon(\boldsymbol{\rho}) - \varepsilon_h(\boldsymbol{\rho}) \right) . \left(\varepsilon(\boldsymbol{\rho}) - \varepsilon_h(\boldsymbol{\rho}) \right) d\Omega \ , \tag{55}$$

and the element average error, Θ_E, as

$$\Theta_{\mathrm{E}} = \frac{1}{\Omega_{\mathrm{E}}} \int_{\Omega_{\mathrm{E}}} \left[D^H(\boldsymbol{\rho}) \right] \left(\varepsilon^*(\boldsymbol{\rho}) - \varepsilon_h(\boldsymbol{\rho}) \right) . \left(\varepsilon^*(\boldsymbol{\rho}) - \varepsilon_h(\boldsymbol{\rho}) \right) d\Omega_{\mathrm{E}} \ . \tag{56}$$

The strategy adopted to verify if a given element should be refined or not, due to the error measure criteria, is given by: if $\Theta_{\mathrm{E}} > (1+\eta)\Theta_{\mathrm{GE}}$, with $\eta > 1$, then we refine the element.

5 ALGORITHM

We are using a bound constrained Truncated-Newton method. The Truncated-Newton method is preconditioned by a limited-memory Quasi-Newton method with a further diagonal scaling. Similar results were obtained with the TANGO algorithm of Andreani *et al* (2004), Andreani *et al* (2005) and Birgin and Martinez (2002).

6 NUMERICAL APPLICATIONS

6.1 Problem Case (1)

Here we consider the problem illustrated in Figure 6, which the material properties (stainless steel AISI 304) to be given as: Young Modulus $E = 193\,GPa$, Poisson's ratio $\nu = 0.29$. The distributed load, $\mathrm{t} = 207{,}000\,kN/m$. The reference temperature of the body is $T_R = 20\,°C$, the temperature of the fluid is $T_f = 25\,°C$ and the prescribed temperature at the clamped edge is $T_p = 100\,°C$. The yield stress, $S_y = 207\,MPa$. The heat conductivity of the material, $k = 16.6\ W/m\,°C$. The coefficient $\beta = 17 \times 10^{-6}\ m/m\,°C$. The convection heat transfer coefficient, $h = 5\ W/m^2\,°C$.

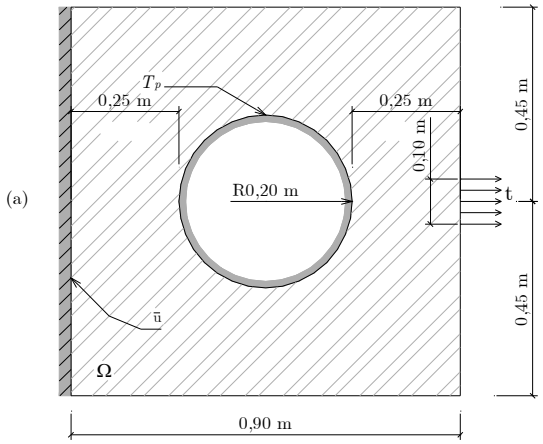

Fig. 6: Definition of the Problem Case (1).

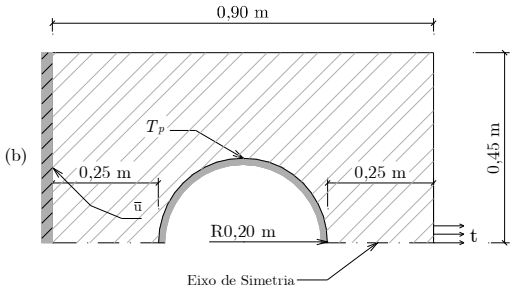

Fig. 7: Symmetrical model of the Problem Case (1) to be solved.

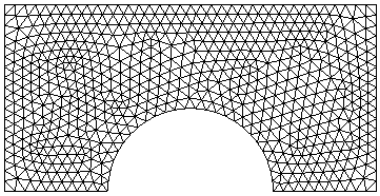

Fig. 8: Initial mesh with 1201 elements and 660 nodes.

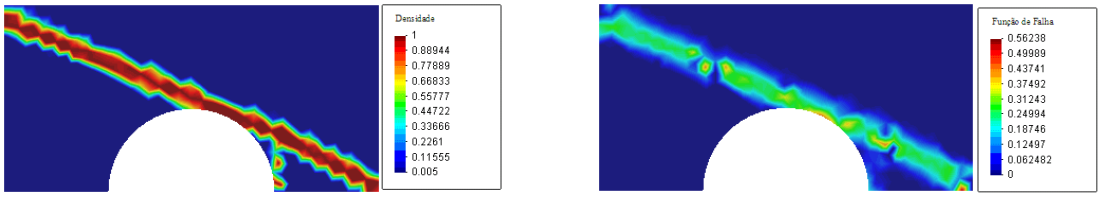

Fig. 9: Results of initial mesh with 1201 elements and 660 nodes only in the symmetrical half, optimum mass distribution and failure function respectively.

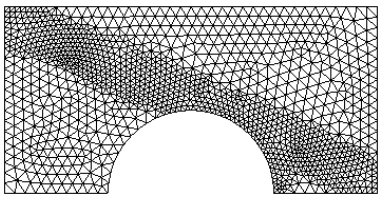

Fig. 10: First h-refined mesh with 2298 elements and 1224 nodes.

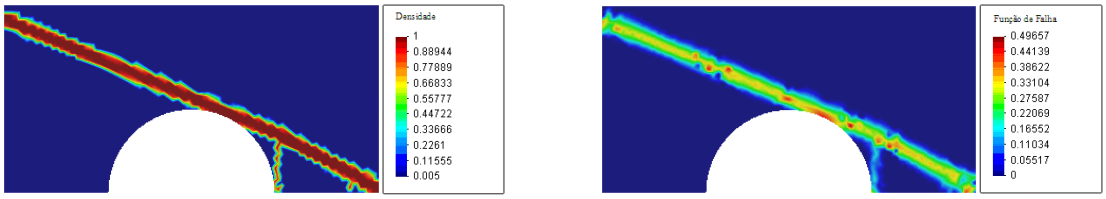

Fig. 11: Results of first h-refined mesh with 2298 elements and 1224 nodes only in the symmetrical half, optimum mass distribution and failure function respectively.

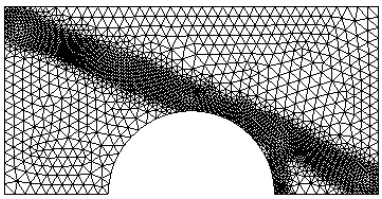

Fig. 12: Second h-refined mesh with 5172 elements and 2684 nodes.

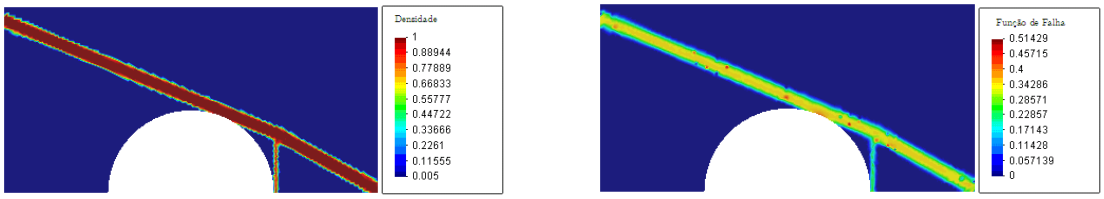

Fig. 13: Results of second h-refined mesh with 5172 elements and 2684 nodes only in the symmetrical half, optimum mass distribution and failure function respectively.

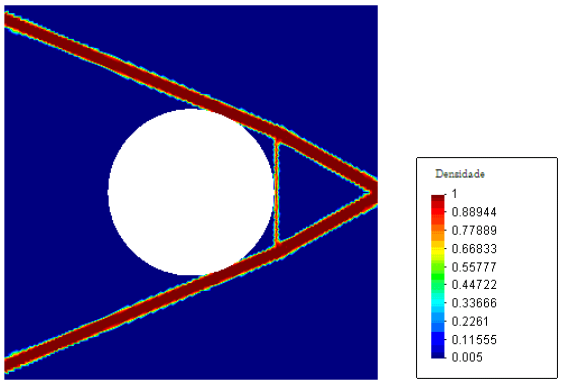

Fig. 14: Representation of optimum topology with 10344 tri3 elements.

6.2 Problem Case (2)

Here we consider the problem illustrated in Figure 15, which the material properties (stainless steel AISI 304) to be given as: Young Modulus $E = 193 GPa$, Poisson's ratio $\nu = 0.29$. The distributed load, $t = 207,000 kN/m$. The reference temperature of the body is $T_R = 20°C$, the temperature of the fluid is $T_f = 25°C$ and the prescribed temperature at the clamped edge is $T_p = 100°C$. The yield stress, $S_y = 207 MPa$. The heat conductivity of the

material, $k = 16.6\ W/m°C$. The coefficient $\beta = 17\times10^{-6}\ m/m°C$. The convection heat transfer coefficient, $h = 5\ W/m^2\ °C$.

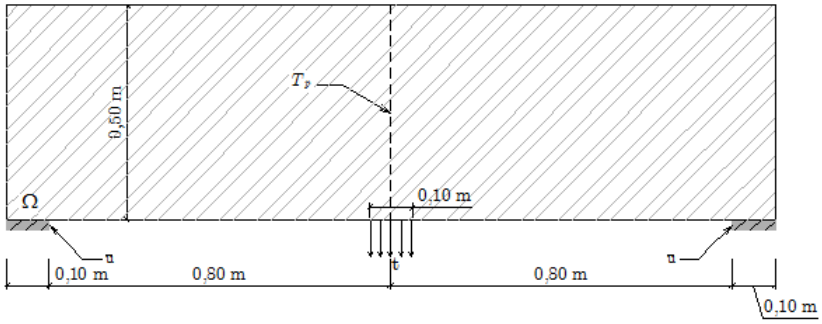

Fig. 15: Definition of the Problem Case (2).

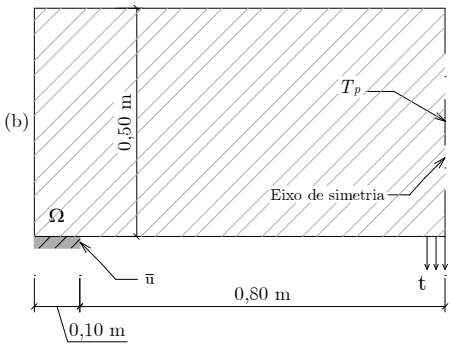

Fig. 16: Symmetrical Model of the Problem Case (2) to be solved.

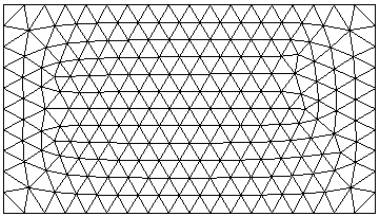

Fig. 17: Initial mesh with 416 elements and 237 nodes.

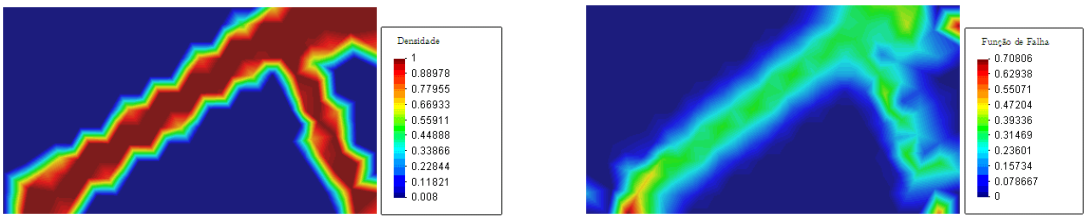

Fig. 18: Results of initial mesh with 416 elements and 237 nodes only in the symmetrical half, optimum mass distribution and failure function, respectively.

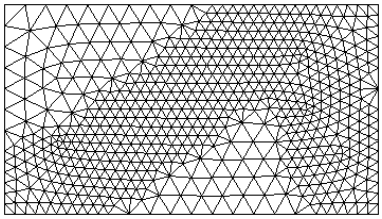

Fig. 19: First h-refined mesh with 1193 elements and 639 nodes.

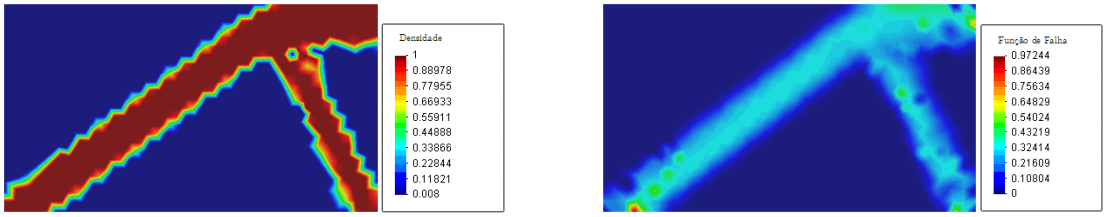

Fig. 20: Results of first h-refined mesh with 1193 elements and 639 nodes only in the symmetrical half, optimum mass distribution and failure function, respectively.

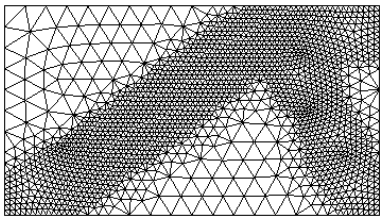

Fig. 21: Second h-refined mesh with 3505 elements and 1814 nodes.

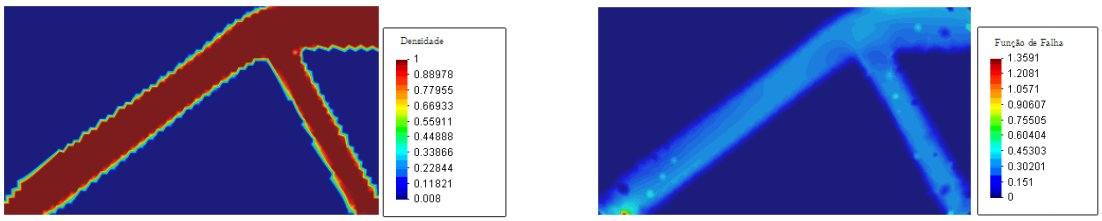

Fig. 22: Results of second h-refined mesh with 3505 elements and 1814 nodes only in the symmetrical half, optimum mass distribution and failure function, respectively.

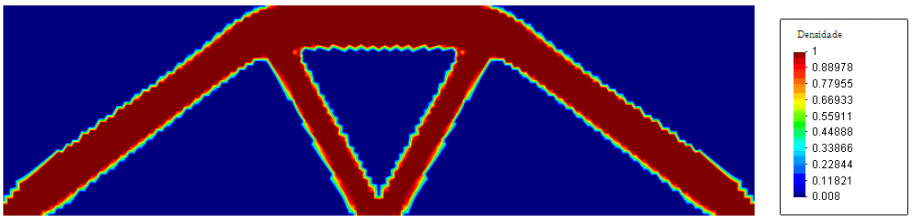

Fig. 23: Representation of optimum topology with 7010 tri3 elements.

6.3 Problem Case (3)

Here we consider the problem illustrated in Figure 24, which the material properties (stainless steel AISI 304) to be given as: Young Modulus $E = 193 GPa$, Poisson's ratio $\nu = 0.29$. The distributed load, $t = 207,000 kN/m$. The reference temperature of the body is $T_R = 20°C$, the temperature of the fluid is $T_f = 25°C$ and the prescribed temperature at the

clamped edge is $T_p = 100\,°C$. The yield stress, $S_y = 207\,MPa$. The heat conductivity of the material, $k = 16.6\,W/m°C$. The coefficient $\beta = 17\times10^{-6}\ m/m°C$. The convection heat transfer coefficient, $h = 5\,W/m^2\,°C$.

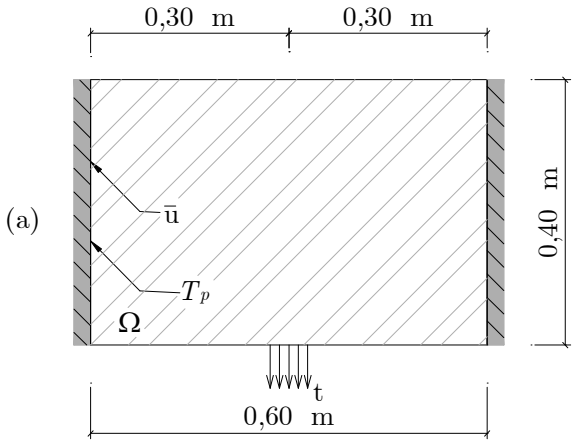

Fig. 24: Definition of the Problem Case (3).

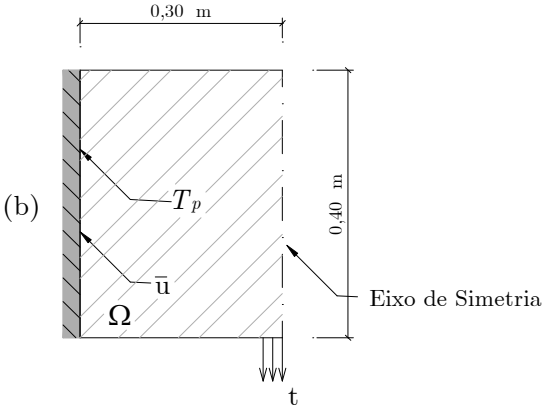

Fig. 25: Symmetrical Model of the Problem Case (3) to be solved.

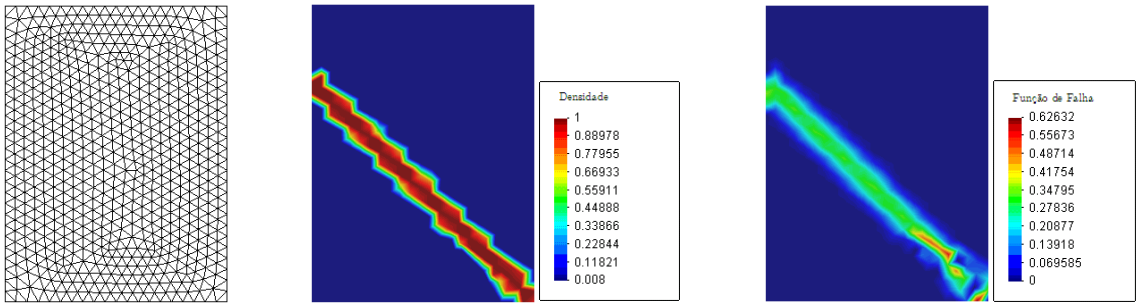

Fig. 26: Initial mesh with 316 elements and 185 nodes only in the symmetrical half, results of optimum mass distribution and failure function, respectively.

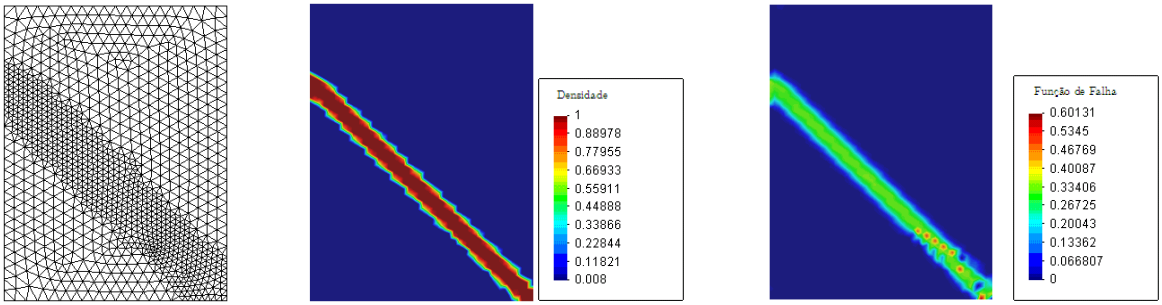

Fig. 27: Second h-refined mesh with 991 elements and 538 nodes only in the symmetrical half, results of optimum mass distribution and failure function, respectively.

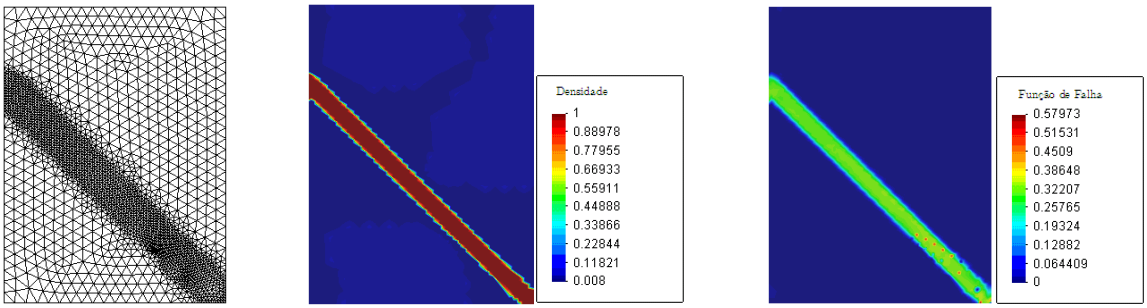

Fig. 28: Third h-refined mesh with 3316 elements and 1725 nodes only in the symmetrical half, results of optimum mass distribution and failure function, respectively.

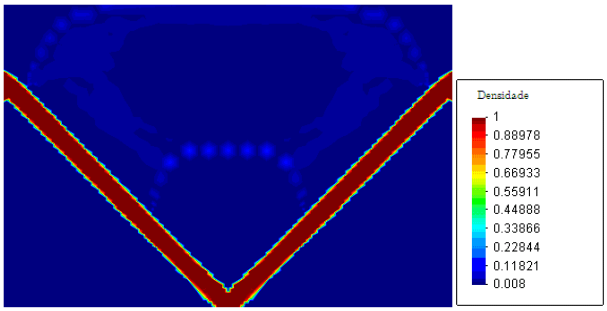

Fig. 29: Representation of optimum topology at the fourth level of h-refinement with 12178 tri3 elements.

7 CONCLUSION

The usage of a multigrid approach or remeshing procedure is important to increase the rate of convergence to the optimum layout of the problem. With this approach, we are able to handle problem with a large number of design variables.

The usage of a non-uniform refinement has shown to decrease the number of design variables and this decrease becomes even more relevant if we refine the problem with a very large number of elements, Carey (1997).

The results were promising, given the stress constraint and tested in meshes with few elements, but for a sharp optimum layout require a very refined mesh, suggesting high computational cost. Hence, the implementation of an adaptive process of refinement was very prudent.

One of the disadvantages of the adopted approach is that we need to determine the element matrices and vectors what increase the computational cost when compared with the pixel type of strategy employed by many Authors. However, the pixel approach requires a refined mesh in order to describe the material boundary with some precision.

8 REFERENCES

Alves, M.K. and Alves, B.K., 1999 “Topology Optimization of Elastic Structures”, IV Congresso Iberoamericano de Engenharia Mecânica, CIDIM 99, Vol.2 - Mecânica dos Sólidos, Santiago, Chile.

Andreani, R.; Birgin, E.G.; Martínez, J.M. and Schuverdt, M.L., 2004 "Augmented Lagrangian methods under the Constant Positive Linear Dependence constraint qualification", Mathematical Programming.

Andreani, R.; Birgin, E.G.; Martínez, J.M. and Schuverdt, M.L., 2005 "On Augmented Lagrangian methods with general lower-level constraints", Technical Report MCDO-050304, Department of Applied Mathematics, UNICAMP, Brazil.

Bendsoe M.P. and Kikuchi N., 1998, “Generating Optimal Topologies in Structural Design Using a Homogenization Method”. Comp. Meth. Appl. Mechs. Engrg., 71, 197-224.

Bendsoe, M.P. and Sigmund, O., 2003, “Topology Optimization: Theory, Methods and Applications”, Springer, New York, 2nd ed.

Bendsoe, M.P. and Rodrigues, H.C., 1991, “Integrated Topology and Boundary Shape Optimization of 2-D solids”, Comp. Meth. Appl. Mech. Engng., 87,15-34.

Bendsoe, M.P.; Díaz, A.R. and Kikuchi, N., 1993, “Topology and Generalized Layout Optimization of Elastic Structures”, Loc. Cit. Bendsoe and Mota Soares, 159-206.

Bendsoe, M.P., 1995, “Optimization of Structural Topology, Shape, and Material”, Springer-Verlag.

Birgin, E.G. and Martínez, J.M., 2002 "Large-scale active-set box-constrained optimization method with spectral projected gradients", Computational Optimization and Applications 23, pp. 101-125.

Brahim-Otsmane, S.; Francfort, G.A. and Murat F., 1989, “Homogenization in Thermoelasticity”, Publications du Laboratoire d´Ánalyse Numérique, Universite Pierre et Marie Curie, Centre National de la Recherche Scientifique, R89011.

Carey, G.F., 1997, “Computational Grids: Generation, Adaptation and Solution Strategies”, Taylor & Francis.

Cho, S. and Choi J.Y., 2005, “Efficient Topology Optimization of Thermo-Elasticity Problems Using Coupled Field Adjoint Sensitivity Analysis Method”, Finite Elements in Analysis and Design, 41, 1481–1495.

Costa Jr, J.C.A. and Alves, M.K., 2003, “Layout Optimization with *h*-adaptivity of Structures”, Int. J. Numer. Meth. Engng; John Wiley & Sons, 58: 83–102.

Duysinx, P., 1998, “Topology Optimization with Different Stress Limits in Tension and Compression”, International report: Robotics and Automation, Institute of Mechanics, University of Liège, Liège, Belgium.

Duysinx, P. and Sigmund, O., 1998, “New Developmets in Handling Stress Constraints in Optimal Material Distribution”, 7th AIAA/USAF/NASA/ISSMO symposium on Multidisciplinary Design Optimization, Saint Louis, Missouri, USA.

Duysinx, P. and Bendsoe, M.P., 1998, “Topology Optimization of Continuum Structures with Local Stress Constraints”, Int. Jnl of Num. Meth. In Eng., vol 43, pp.1453-1478.

Francfort, G.A., 1983, “Homogenization and Linear Thermoelasticity”, SIAM J. Math. Anal., 14, 696-708.

Kikuchi, N. and Suzuki, K., 1992, “Structural Optimization of a Linearly Elastic Structure using the Homogenization Method”, Inc. Cit. Rozvany, 1992, 199-242.

Petersson, J. and Sigmund, O., 1998, “Slope constrained topology optimization”, Int. J. Numer. Meth. Engng., 41, 1417-1434.

Rodrigues, H.C. and Fernandes, P., 1993, "Topology Optimization of Linear Elastic Structures Subjected to Thermal Loads", Bc. Cit. Bendsoe and Mota Soares, 437-450.

Sigmund, O. and Petersson, J., 1998, "Numerical instabilities in topology optimization: a survey on procedures dealing with checkerboards, mesh dependencies and local minima". Structural Optimization, vol. 16. Springer-Verlag: Berlin, 68–75.

Silva, P.S.R., 2007, "Estruturas Termoelásticas sob Otimização Topológica e *H*-adaptatividade", MSc. Dissertation, Post-graduate Program of Mechanical Engineering, UFRN, Natal-RN, Brazil.

Suzuki, K. and Kikuchi, N., 1990, "Generalized Layout Optimization of Shape and Topology in Three Dimensional Shell Structures", kept. No.90-05, Dept. Mech. Engrg. and Appl. Mech., Comp. Mech. Lab., University of Michigan, USA.

Suzuki, K. and Kikuchi, N., 1991, "Shape and Topology Optimization for Generalized Layout Problems Using the Homogenization Method". Comp. Meth. Appl. Mechs, Engng., 93, 291-318.

Zienkiewicz, O.C. & Zhu, J.Z., 1990, "The three R's of engineering analysis and error estimation and adaptivity", Comput. Methods Appl. Mech. Engrg., 82, 95-113.

Zienkiewicz, O.C. & Zhu, J.Z., 1991, "Adaptivity and mesh generation", Int. J. Numer. Meth. Engng., 32, 783-810.

9 RESPONSIBILITY NOTICE

The authors are the only responsible for the printed material included in this paper.